Tellus (1977) *29*, 25–40

The composite structure of the monsoon depression

By R. V. GODBOLE, *Florida State University, Tallahassee, Florida 32306, USA*

(Manuscript received November 24, 1975; in final form March 29, 1976)

ABSTRACT

A composite three dimensional structure of the monsoon depression has been constructed using five monsoon depression cases of 1973. The parameters considered for compositing are wind components, temperature, relative humidity, surface pressure, cloud cover and precipitation. The distributions of these parameters are obtained with respect to the depression center as origin. The results indicate that the depression is an intense low pressure system with a central pressure of 990 mb. The associated circulation is very vigorous. Strongest winds of about 50 kts are noted in the southwest. The analyses of the pressure and wind fields suggest that the horizontal scale of the depression is about 1500 km. The field of temperature anomaly clearly brings out the cold core structure of the depression. The precipitation pattern shows that the rainfall rates exceeding 120 mm in 24 hrs occur to the west of the depression.

The vertical cross-sections through the center of the depression of horizontal wind components indicate that the depression is confined to the lower troposphere from the surface up to 400 mb. The region ahead of the depression is characterized by strong cyclonic vorticity, convergence and upward motion. Relatively weak anticyclonic vorticity, divergence and subsidence are noted behind the depression.

Introduction

Monsoon depressions form at the head of the Bay of Bengal during the monsoon season from June to September. These depressions, like other tropical disturbances, move westward having a life cycle of 3 to 5 days. The number of depressions per month and their tracks vary from year-to-year, but on an average, two depressions per month form and move west-northwestward merging with the seasonal heat low over northwest India. Although these depressions do not normally reach hurricane intensity, surface winds of over 40 kts have been frequently reported. Satellite photographs show that over the north Bay of Bengal where these depressions originate, cloud clusters are usually present which are similar to those associated with pre-hurricane depressions over the tropical Atlantic and Pacific Oceans. One of the reasons for the monsoon depressions not becoming hurricanes is the presence of strong easterly vertical shear which is not favorable for their further development into hurricanes. Also, since these depressions do not stay long over the Bay of Bengal, these are not able to derive the massive amount of sensible heat from the sea necessary for the growth of the tropical storm. Heavy rainfall is the most outstanding phenomenon associated with these depressions. Amounts up to 300 to 400 mm of rain in 24 hours have been recorded. The monsoon depression is thus an interesting tropical disturbance in regard to its intensity and associated rainfall rates. Its presence or absence has important implications from the point of view of drought conditions over the monsoon domain.

Numerous synoptic and diagnostic case studies of individual monsoon depressions are found in the literature (Das, 1952; Pisharoty & Asnani, 1957; Ananthakrishnan & Bhatia, 1958; Koteswaram & George, 1958; Bedekar & Benerjii, 1958; Rao & Rajamani, 1972). In our recent study (Krishnamurti et al., 1975) we made an attempt to examine a single case study of August 1968 in all its aspects such as observational, diagnostic, prognostic and energetics. Studies along other lines, such as the importance of radiative effects over the monsoon domain through complex cloud structure using other case studies are already under way. While working on these different case studies and especially dealing with the problem of energetics, we felt the need to know the mean structure of the monsoon depression and its behavior during its life cycle of 2 to 3 days. The present study is the outgrowth of this demand and deals with the composite structure of the monsoon depression. The valuable information yielded by compositing technique on disturbances in other parts of the tropics (Williams, 1970; Reed & Recker, 1971; Frank, 1975) prompted us to apply it to the monsoon depression which, like other tropical disturbances, suffers from having a good data coverage especially over the North Bay of Bengal—their place of origin. We also feel that such a study is very important at this stage when planning and organizing of MONEX-1979 is in progress and which has monsoon depression as one of the principal scientific programs for investigation.

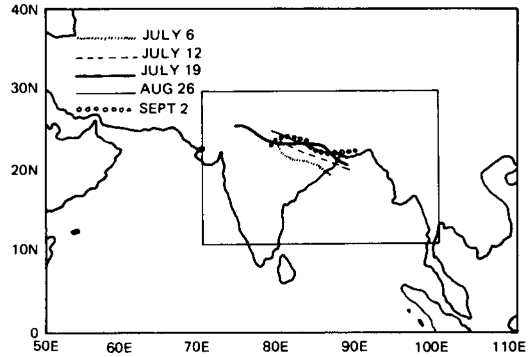

Fig. 1. The region considered for collecting the data for compositing and the tracks of five monsoon depressions of 1973. The inner domain is used for the analysis of the data.

Sources of data

Data for the following monsoon depressions of 1973 were used for compositing.

1.	July 6, 12Z	to	July 9, 00Z
2.	July 12, 00Z	to	July 14, 12Z
3.	July 19, 00Z	to	July 22, 12Z
4.	Aug 26, 00Z	to	Aug. 31, 12Z
5.	Sept 2, 12Z	to	Sept 5, 00Z

The tracks of these depressions and the region considered are shown in Fig. 1. Winds, temperature and dew-point values were collected at the surface and at 850, 700, 500, 300 and 200 mb. Also collected were the data for surface pressure, cloud cover and precipitations. The primary source of data came from the analyzed charts supplied by the Indian Ocean and Southern Hemispheric Analyses Center of the Meteorological Office at Poona in India. This was further supplemented by the Global Telecommunication System data obtained from the National Center for Atmospheric Research. The aircraft data was provided by the Regional Meteorological Center at Bombay. Additional aerological data for the region of Arabia and Africa were obtained from the analyzed charts provided by the Sudan Meteorological Service.

The outer domain of Fig. 1 was originally used for another on-going study on the monsoon depressions which involve the application of the Florida State University Tropical Prediction model. All the available data in this domain (about 80–120 upper air and 100–120 surface observations) have been utilized for compositing.

The inner domain shown in the figure is the one actually used for analysis and presenting the results in this study. However, while working on the energetics of the present study, we felt that by considering a small domain, we were neglecting one important aspect, namely, the energy interaction between the disturbance and the main monsoon circulation. If we are to talk about anything meaningful about the role of various energy interaction terms in respect to monsoon disturbance *vis-à-vis* monsoon circulation, we ought to consider a larger domain of Fig. 1. This is being done and it will be a subject of another study to be reported subsequently. In any case, for merely examining the observational structure of the monsoon depression derived from the compositing technique, the choice of a smaller domain of Fig. 1 may be justified.

Method of compositing and analyses

If we consider that all the observations at one synoptic time correspond to one set, there are in all 38 sets of observations covered by the five depressions. Each set has approximately 80–120 observations for upper air and 100–120 observations for the surface. This makes, on an average, a total of 3800 upper air and 4500 surface observations that went into the compositing. All these sets (of observations) were put together for compositing irrespective of the stages of development of the disturbance such as the formative stage, the mature stage and the decay stage. This is done mainly because we are essentially interested, at this time, in knowing the mean picture of the monsoon depression during its life cycle. With 38 sets of observations, the mean location of the depression center turns out to be at 23° N and 83° E.

For each set of observations, the center of the depression is assigned both *X*- and *Y*-coordinates as zero. All the stations are then re-identified in terms of distance (in degrees of latitude and longitude) with respect to the depression center as origin. The revised latitude and longitude of stations falling within one degree have been rounded off to a whole degree. In other words, a one degree mesh with respect to storm center as origin is generated and data from stations lying in the same one degree latitude–longitude box are averaged over as representative of that box. The parameters considered for compositing are winds, temperature, surface pressure, cloud cover and precipitation. A typical example of the total number of wind observations (1275 for the 850-mb level) that emerged from the compositing is shown in Fig. 2. The composite data thus obtained were then analyzed. As already mentioned, the analysis was restricted to a smaller domain of Fig. 1.

For analysis of the above parameters, raw data from the composite did not always yield a smooth field. For example, the wind field at and below 500 mb was quite smooth but not at 300 and 200 mb clearly suggesting that the disturbance has no influence whatsoever at these levels. It is a known fact that the wind fields at these higher levels are largely dominated by the semipermanent Asiatic anticyclone. Again in the horizontal, the wind field was smooth within the radius of 5–8 degrees of longitude from the depression center, thus delineating the horizontal radius of influence of the disturbance. As a matter of fact, this was the main consideration in limiting our analysis to the smaller domain shown in Fig. 1. Next in line of smoothness were the fields of precipitation, cloud cover, surface pressure, temperature and lastly, the specific humidity. It is obvious that the distribution of temperature and moisture in the lower troposphere depends to a great extent upon the presence

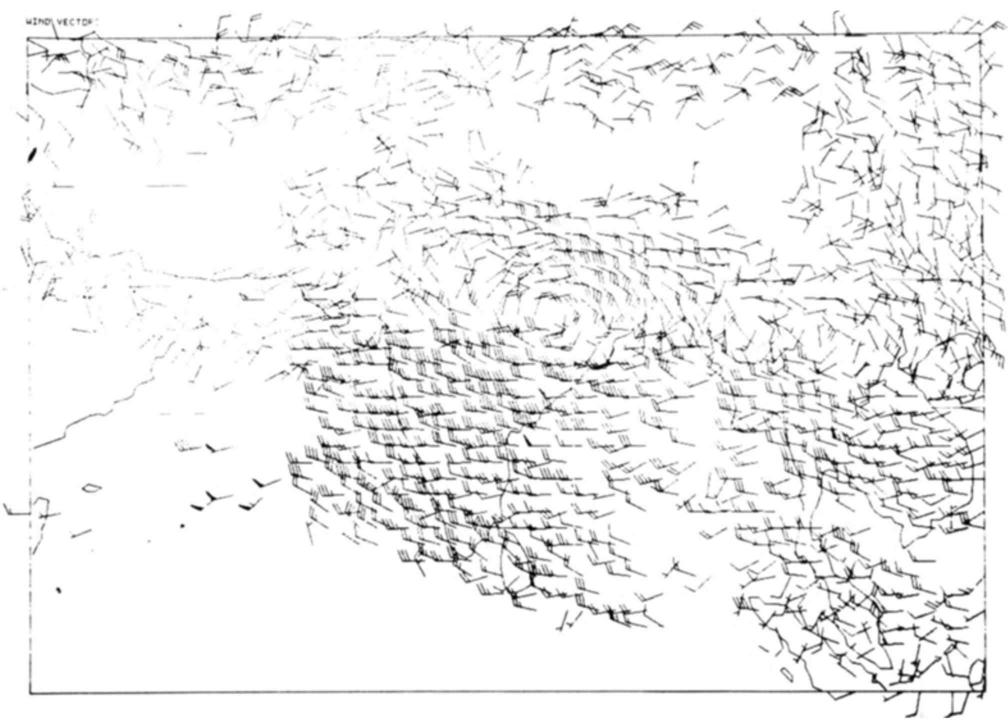

Fig. 2. A typical example of the 850 mb composite data at one degree latitude–longitude grid with the depression center as the origin.

of oceans and continents. As such, this further narrows down the radius of influence of the depression as far as the temperature and moisture parameters are concerned.

Analysis of winds was done by the method of objective analysis following Tripoli & Krishnamurti (1975). The method is slightly modified so as to incorporate a correction to aircraft winds due to vertical wind shear. Analysis of other parameters was done subjectively invoking a certain degree of smoothing wherever necessary. In order to maintain the consistency with the prognostic studies at hand, the final analyses of the horizontal components of wind (u, v) were done for the surface and 800, 600, 400 and 200 mb levels. Temperature and specific humidity were analyzed at the surface and 900, 700, 500 and 300 mb whereas the vertical velocity was analyzed for 900, 700, 500 and 300 mb levels.

Results and discussion

Surface pressure

The mean surface pressure field is illustrated in Fig. 3. There is a planetary scale monsoon trough

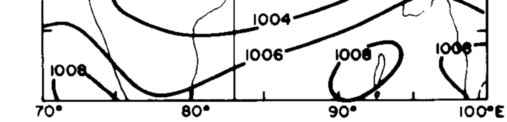

Fig. 3. Spatial distribution of the composite surface pressure (mb).

that stretches across the Indian sub-continent in the northwest-southeast direction. The trough has a mean pressure of about 996 mb. On the synoptic chart, this trough is normally found to extend from the west coast of Africa to the east coast of Asia. The monsoon depression which is a synoptic scale disturbance has a central pressure of 990 mb and is embedded in the monsoon trough. In some individual cases, central pressure of as low as 986 mb have been reported. Evidently, the monsoon depression is an intense low pressure system as compared to other tropical disturbances.

There appears to be a close linkage between the monsoon trough (planetary scale) and the monsoon depression (synoptic scale); the trough offering a track for the depression to ride along. Prior to the formation of the monsoon depression, the trough tends to shift south of its mean position. At this stage, it may be only the eastern half of the trough that has shifted southward. When the depression propagates farther west, the trough begins to revert back to its mean seasonal position (Srinivasan et al. 1971). It is a known fact that when the trough shifts northward farther away from its mean position to the foot-hills of the Himalayas, monsoon depressions do not form over the north Bay of Bengal.

Winds

The streamline and isotach fields of the wind at the surface and at 800, 600, 400 and 200 mb are shown in Figs. 4a through 4e. For convenience, lines are drawn along the latitude and longitude through the mean position of the depression center (i.e. 23° N and 83° E) in order to examine the flow field with respect to various sectors around the storm center. It is seen from the figures that the cyclonic circulation is well-defined in the lower and middle troposphere. The westerly and southwesterly flow to the south of the depression is predominantly stronger than the flow to the north. It may be noted that the broad monsoon current over the region during the monsoon season is southwesterly to the south of the monsoon trough and easterly and southeasterly to the north of it. The circulation associated with the monsoon depression, thus, accentuates the basic monsoon flow. At the surface (Fig. 4a), the flow to the south of the depression attains a maximum intensity of 7.5 m sec^{-1} in the southwestern sector. To the north of the depression, the flow reaches a peak intensity of 5 m sec^{-1}. Here, strong winds are concentrated over a relatively small area in the northeastern sector somewhat close to the storm center. At 800 mb, the pattern of the motion field is very much similar to that at the surface. The circulation is more vigorous at this level. Winds have maximum speed of 20 m sec^{-1} to the south and 15 m sec^{-1} to the north of the depression. At 600

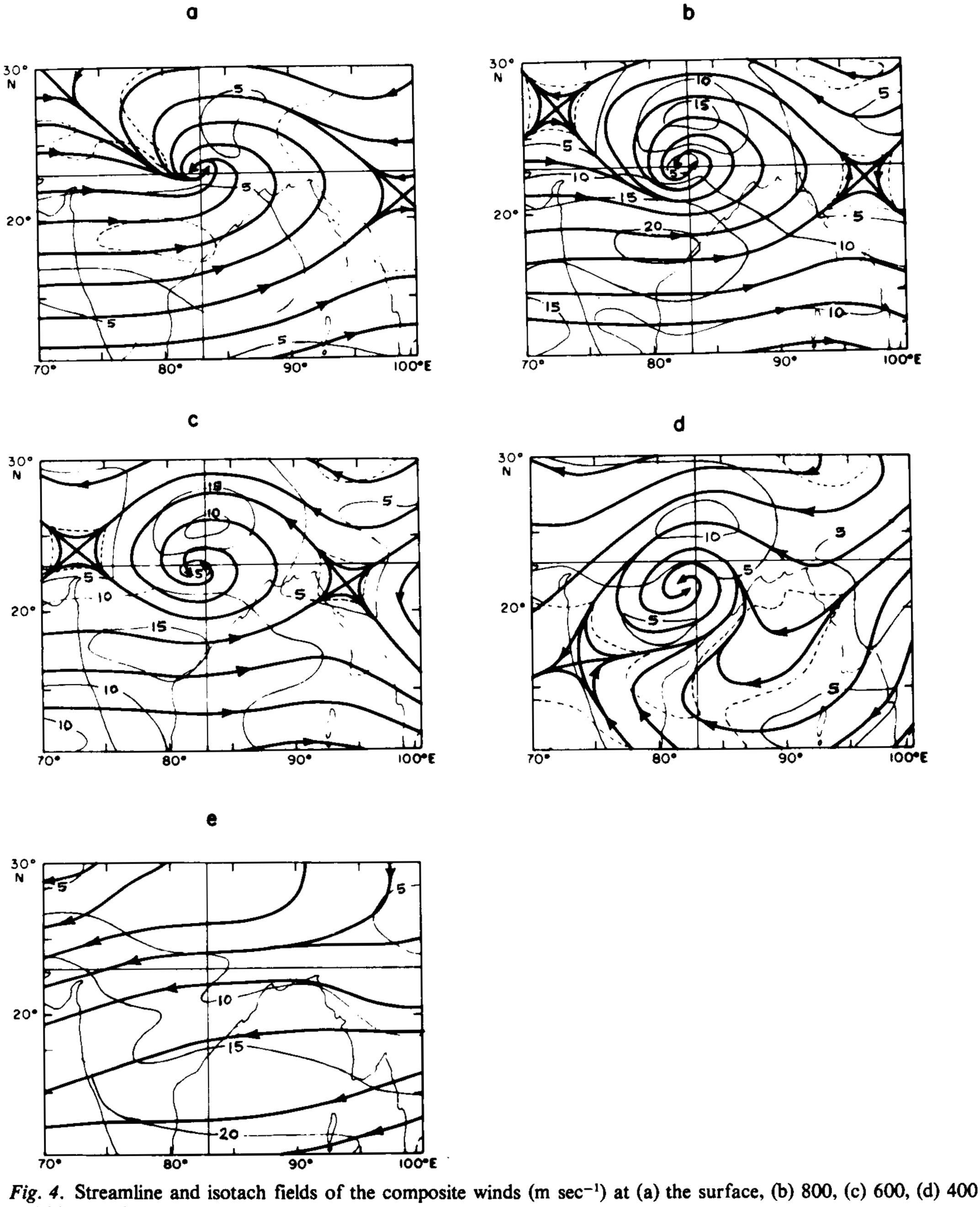

Fig. 4. Streamline and isotach fields of the composite winds (m sec^{-1}) at (a) the surface, (b) 800, (c) 600, (d) 400 and (e) 200 mb.

and 400 mb (Fig. 4c and 4d), the circulation shows the weakening of winds with height. The motion field at 400 mb has many interesting features because it marks, more or less, the transition level where the influence of the upper tropospheric anticyclone begins to appear in the northern latitudes. At this level, the depression center is shifted southwestward from its surface location and the flow to the north of the depression is stronger than that to its south. At 200 millibars, the flow becomes predominantly zonal due to the influence of the Tibetan anticyclone.

The variation of zonal and meridional winds with height is portrayed in Figs. 5a and 5b respectively. For constructing these vertical cross sections, wind information at the standard isobaric levels has also been used. The cross section for the zonal wind is along 83° E through the depression center (Fig. 5a). The zonal westerlies reach a peak intensity of 20 m sec^{-1} at 800 mb. The transition from westerlies to easterlies takes place at about 400 mb which marks the limit of the vertical extent of the depression. Above 400 mb, the easterlies strengthen with height. To the north of the depression, the easterlies with maximum speed of 15 m sec^{-1} occur over a greater depth (850–500 mb) than the westerlies to the south. For meridional wind, the cross section is drawn along 23° N (Fig. 5b). Southerlies to the east attain a maximum speed of 10 m sec^{-1} at 850 mb. The northerlies to the west also reach a peak intensity of 10 m sec^{-1} and although this maximum appears to occur at 500 mb in the figure, there is a secondary maximum at 800 mb as is evident from Fig. 4b. At any rate, the flow pattern shown in Fig. 5b suggests that the monsoon depression is characterized by a northward transfer of momentum primarily in the lower levels and a return transfer southward at both lower and middle levels.

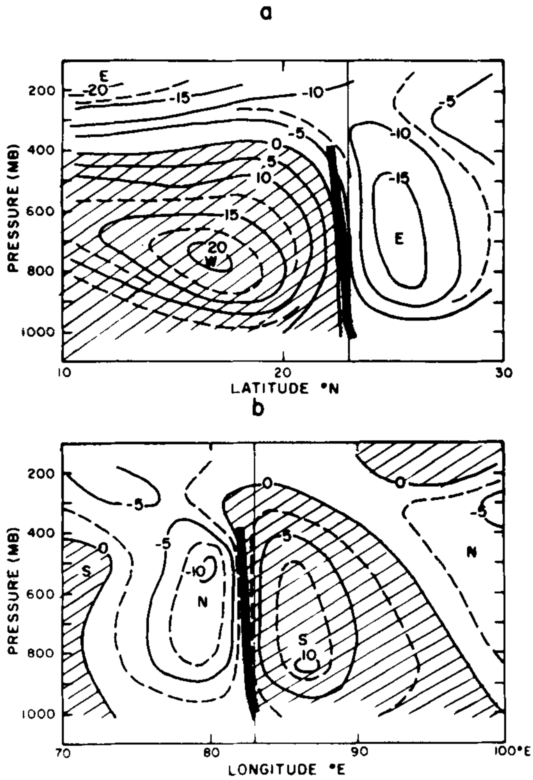

Fig. 5. Vertical cross section of (a) the zonal wind along 83° E, and (b) the meridional wind along 23° N (m sec^{-1}). The dark-shaded line represents the axis of the depression in the wind field.

The broad hatched line in Fig. 5 represents the axis of the monsoon depression along the vertical. This axis has a slight tilt to the southwest with height. This is opposite to our earlier findings (Krishnamurti et al., 1975) which indicated an eastward tilt with height. Our earlier results were pertaining to only a single case study. However, since our present results are in conflict with our earlier results, we examined this question of the tilt of the axis by inspecting individual sets of observations for each synoptic time. We noticed that there were as many sets with eastward tilts as those with westward tilts. This naturally leads one to the inference that the monsoon depressions do not exhibit a well-marked tilt along the vertical, at least in the wind field. Keshavmurty (1970) and Murakami (1975) have shown that all monsoon depressions are either nearly vertical or have a small westward tilt with height.

Comparison of the wind field with that obtained by Reed and Recker (1971) for the tropical easterly wave over the eastern Pacific clearly brings out the fact that the monsoon depression is associated with a vigorous circulation.

Temperature

The temperature field is depicted in terms of temperature anomaly which is defined as the deviation of temperature from its latitudinal mean value. Negative temperature anomaly, therefore, represents temperature below its mean value and vice versa. Fig. 6a–e shows the thermal fields at the surface and at 900, 700, 500 and 300 mb. The thermal field clearly brings out the cold core structure of the monsoon depression in the lower troposphere from the surface to 700 mb (Figs. 6a through 6c). While the result corroborates our earlier finding, it is opposite to what has been reported by Keshav-

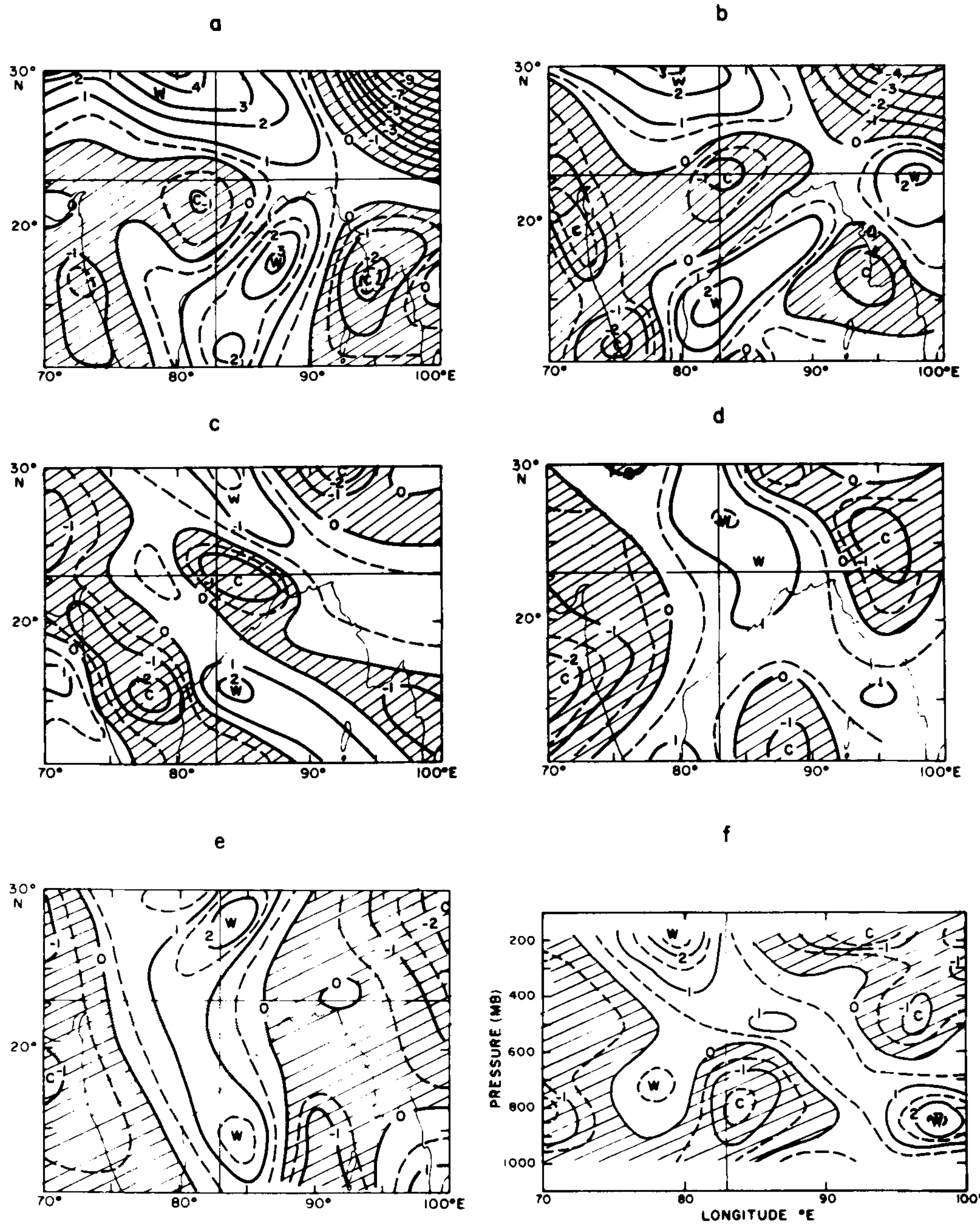

Fig. 6. The distribution of the temperature anomaly (°C) at (a) the surface, (b) 900 mb, (c) 700 mb, (d) 500 mb, (e) 300 mb and (f) the vertical cross of the temperature anomaly along 23° N.

murthy (1970) and Murakami (1975). The cold core is weak (≈ -1 °C) at the surface (Fig. 6a), becomes strong (≈ -1.5 °C) at 900 and 700 mb (Figs. 6b and 6c) and weakens above 700 mb. At 500 and 300 mb (Figs. 6d and 6e), a warm core overlies the low-level cold core with a maximum amplitude of 2 °C at 300 mb.

The complex pattern of the thermal field at the surface (Fig. 6a) especially over the southern-half of the domain, arises mainly due to the presence of continents and oceans. However, one can glean some broad salient features even from this complex pattern. For example, the atmosphere over the Bay of Bengal is warmer than that over the Arabian Sea. It has long been known that the Bay of Bengal which is an active cyclogenetic area has higher sea surface temperature than the Arabian Sea. The very low temperatures in the northeast (i.e., South China) appear to be the characteristic of that region because of high terrain. In the northwest, the warm core is essentially due to the Rajasthan desert.

The vertical cross section of the temperature anomaly is presented in Fig. 6f. The values at the standard isobaric levels have also been utilized for constructing the cross-section. The cold core depression has a maximum amplitude ($\approx -1.6\,^{\circ}$C) at 800 mb. The reversal of the thermal field takes place at about 600 mb. The warm core ahead of the depression is mainly due to the warm air advection of the desert air from the northwest. It is interesting to note that the cold core has an eastward tilt with height which is characteristic of all the tropical disturbances. This indicates that some baroclinic mechanism does play an important part in the development of the monsoon depression.

Moisture

The moisture field is depicted in terms of relative humidity in Figs. 7a through 7d for the surface and 900, 700 and 500 mb. Analysis for the 300-mb level is not presented because of the paucity of data at this level. The outstanding feature of the moisture field is the presence of very moist regime (R.H. $>90\%$) ahead of the depression all through the lower troposphere. It is quite obvious that the dynamical forcing is the cause for this deep moist layer. The topographic effects also cause secondary moist regimes (R.H. $> 90\%$) which are most pronounced at the surface. These regimes are near the Arakans in Barma, Ghats in West India and Assam Hills in northeast India. The dry regime (R.H. $\approx$ 65–70%) over the leeside of the Ghats and over southeast India are the typical features for this region (Rao & Ramamurthy, 1968; Godbole, 1975). The presence of dry air in the northwest is due to the Rajasthan desert and has a depth all the way up to 500 mb.

The vertical cross section of the moisture field is portrayed in Fig. 7e. The deep moist layer ahead of the depression stands out clearly as against the shallow moist layers due to terrain.

Vorticity

The field of relative vorticity is portrayed in Fig. 8 for the surface and 800, 600, 400 and 200 mb levels. At the surface (Fig. 8a), the cyclonic vorticity predominates over most of the domain. Except in the vicinity of the depression, the cyclonic vorticity is weak. For example, values of relative vorticity greater than 1.0×10^{-5} sec^{-1} are concentrated only within a radius of about 300 km from the depression center with a maximum value of 5.0×10^{-5} sec^{-1} sitting right over the center. At higher levels, the cyclonic vorticity gains in strength with height up to about 800 mb (Fig. 8b) and then decreases slowly with height reversing in sign in the upper troposphere. At 200 mb (Fig. 8e), anticyclonic vorticity predominates over most of the domain. It is also seen from the figure that the cyclonic vorticity decreases in its horizontal extent with height and that the zone of maximum vorticity shifts to the west (i.e. ahead) of the depression at higher levels. In the north–south direction ahead of the depression, the cyclonic vorticity is stronger to the south than to the north. In other words, the zone of maximum cyclonic vorticity lies to the southwest of the depression.

The cross section of the relative vorticity in the zonal plane along 23° N is shown in Fig. 8f. The pattern clearly demonstrates the well-organized narrow vertical tube of intense cyclonic vorticity ahead of the depression. Maximum value of 13.0×10^{-5} sec^{-1} occurs in a layer between 700 and 850 mb. The top of the vortex tube extends a little over 400 mb.

Comparison of the vorticity field associated with other tropical disturbances indicates that we are dealing with a cyclonic circulation which is 3–10 times stronger. For example, in the African monsoon cyclone (Pedgley & Krishnamurti, 1975) and in the Caribbean easterly wave (Baumhefner, 1968), the maximum relative vorticity is about 5.0×10^{-5} sec^{-1}; for a composite cloud cluster in the Pacific (Williams, 1970) it is about 3.0×10^{-5} sec^{-1} and for a composite ITCZ wave in the Pacific (Reed & Recker, 1971) it is even much less (1.0×10^{-5} sec^{-1}).

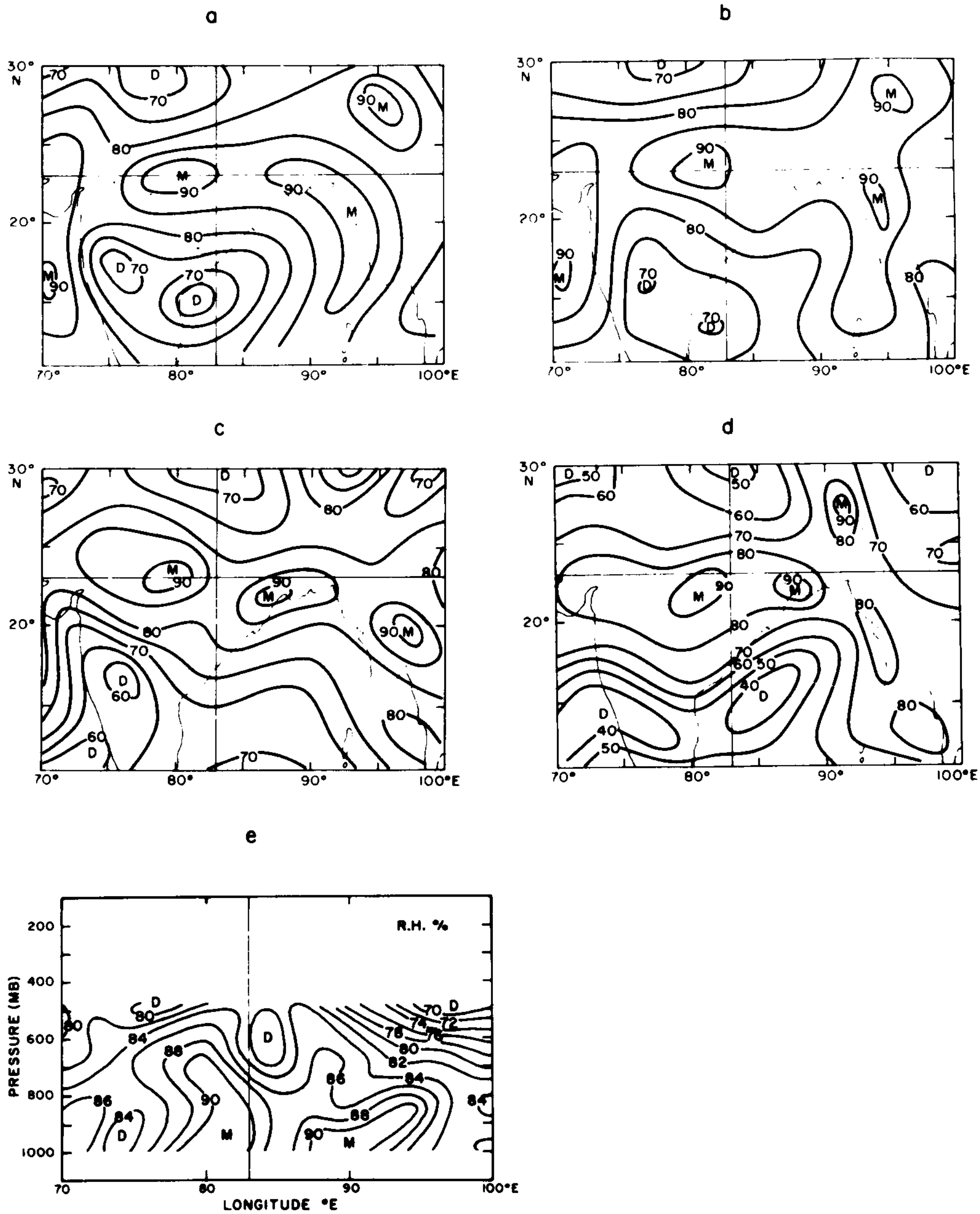

Fig. 7. The distribution of the composite moisture field in terms of relative humidity (%) at (a) the surface, (b) 900 mb, (c) 700 mb, (d) 500 mb, and (e) the vertical cross section of the relative humidity along 23° N.

Divergence

The divergence field is shown in Fig. 9. At the surface (Fig. 9a), there is a convergence in the close vicinity ($\approx$300 km) of the depression. The maximum convergence ($\approx 4.0 \times 10^{-5}$ sec^{-1}) occurs slightly to the northeast of the depression center. Outside the radius influence of the depression ($\sim$5° longitude), the regions of convergence and divergence are interspersed between each other. At 800 and 600 mb (Figs. 9b and 9c) the magnitude of

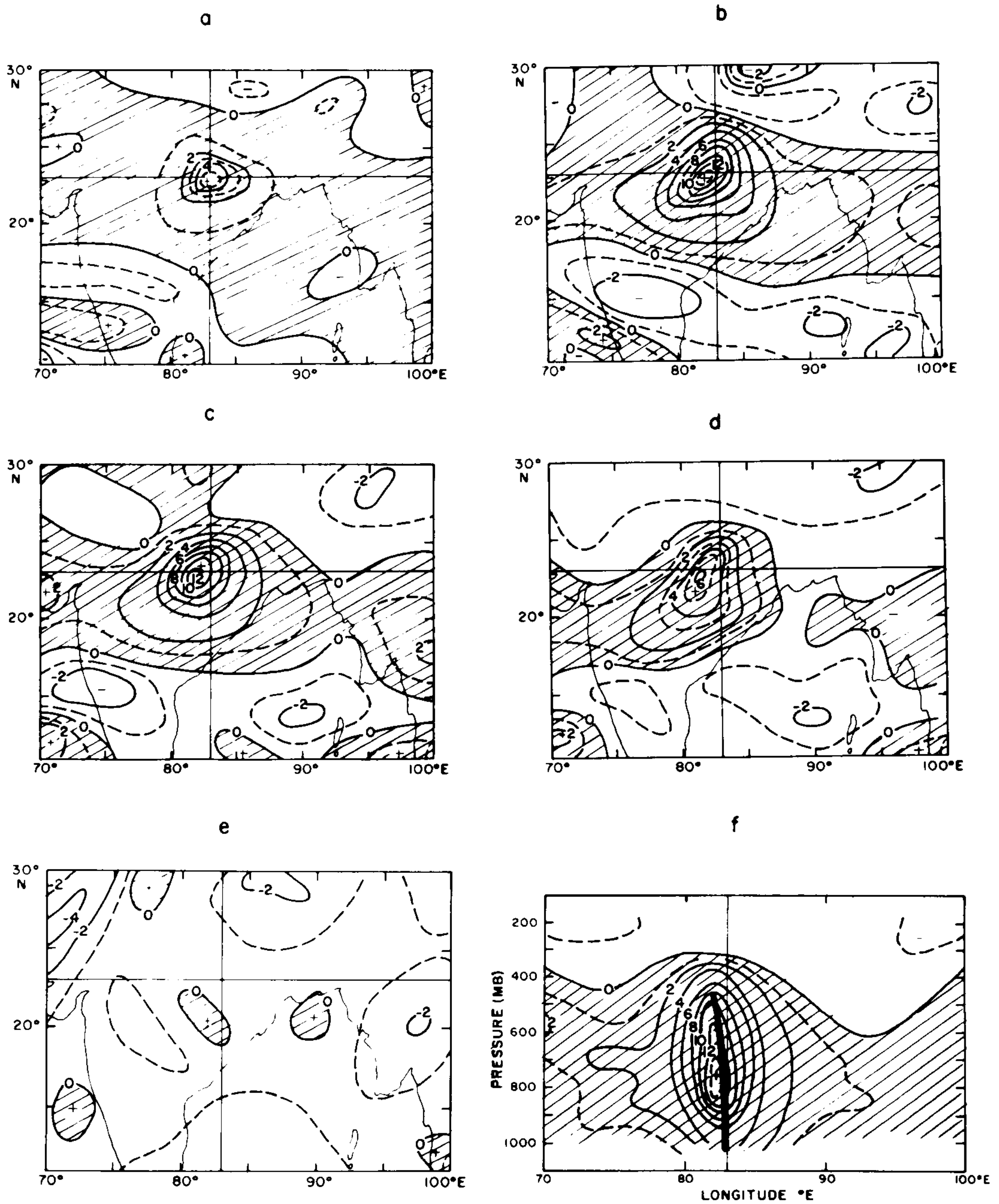

Fig. 8. The distribution of the relative vorticity (10^{-5} sec^{-1}) at (a) the surface, (b) 800 mb, (c) 600 mb, (d) 400 mb, (e) 200 mb, and (f) the vertical cross section of the relative vorticity along 23° N.

the convergence associated with the depression decreases slightly with height. Also, the zone of maximum convergence shifts to the west (i.e. ahead) of the depression center. To the east (i.e. behind) of the depression center there is a weak divergence. In the north–south direction, we find that the convergence is stronger in the north than in the south. The overall effect, therefore, is that

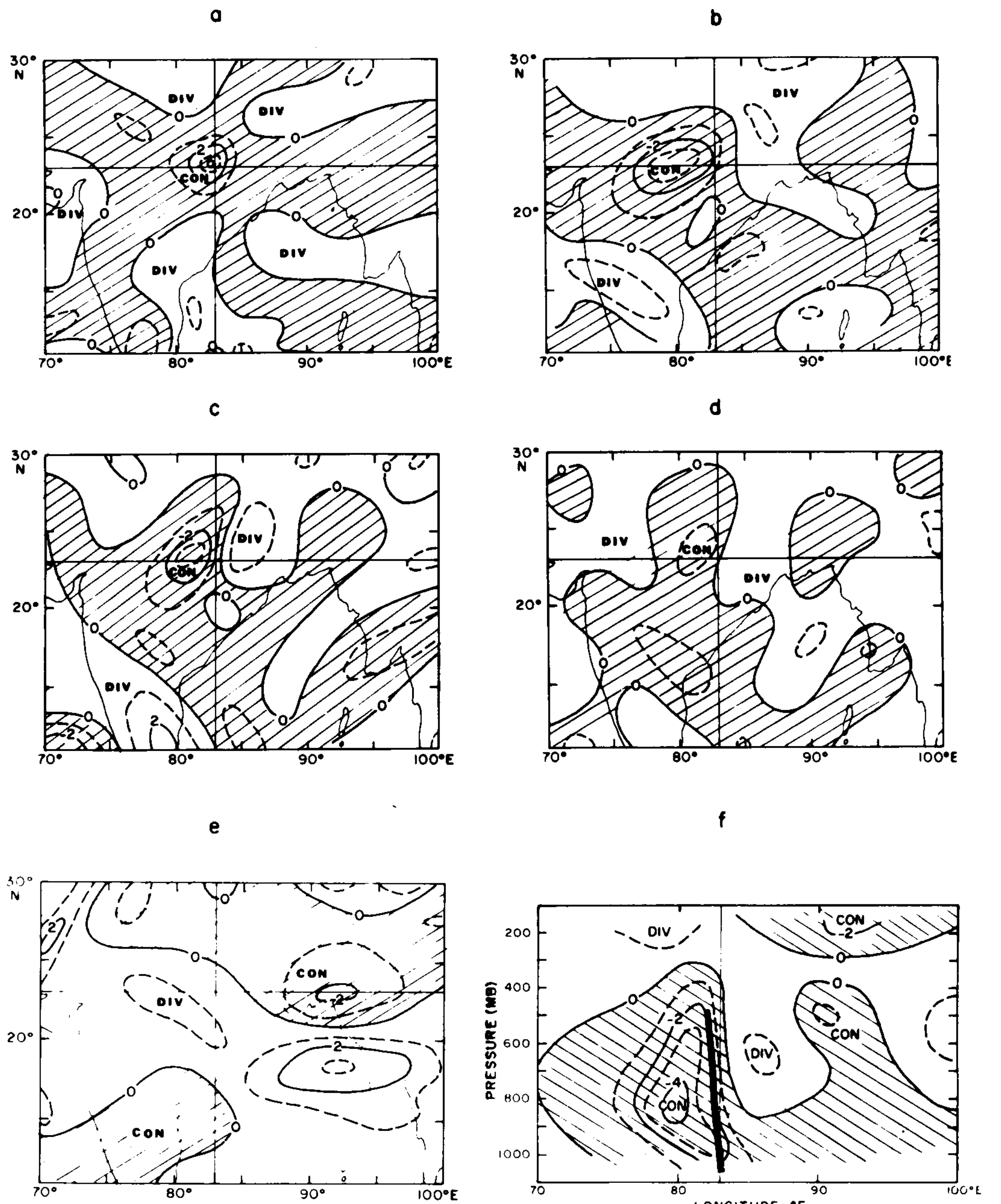

Fig. 9. The distribution of the convergence and divergence (10^{-5} sec^{-1}) at (a) the surface, (b) 800 mb, (c) 600 mb, (d) 400 mb, (e) 200 mb, and (f) the vertical cross section of the field of convergence along 23° N.

pronounced convergence takes place in the northwest sector. This partly explains as to why all the monsoon depressions propagate west-northwestward. At 400 mb (Fig. 9d) the convergence ahead of the storm center is relatively weak ($\approx -1.0 \times 10^{-5}$ sec^{-1}) and the domain, on the whole is more under the influence of the divergence. At 200 mb (Fig. 9e), an area of divergence overlies that of convergence at lower levels as required by the principle of mass compensation.

The vertical cross section of the divergence field along 23° N is shown in Fig. 9f. Ahead of the depression convergence predominates from the surface up to 400 mb. Maximum convergence takes place in a layer from 700 to 900 mb. A rather weak divergence is found behind the depression in the middle and upper troposphere.

Vertical velocity

The vertical velocity field corresponding to the above divergence is portrayed in Fig. 10. For evaluating the vertical velocity, kinematic method is used in which the vertically integrated horizontal divergence is assumed to be zero. The divergence at each level is then adjusted using a simple linear correction technique. For the boundary conditions, the vertical velocity is considered as zero at the surface and at 100 mb. The broad features as seen from Fig. 10 are that there is a band of rising motion running in the northwest-southeast direction through the storm center and two bands of sinking motion on either side. Large values of rising motion are concentrated over the depression area. At 900 mb (Fig. 10a), the upward motion has a maximum value of 25×10^{-4} mb sec^{-1} occurring just to the northwest of the depression center. The downward motion in the northeast as well as in the southwest is relatively weak. At higher levels the pattern broadly remains unchanged except that the zone of maximum upward motion shifts to the west of the depression center. The upward motion ahead of the storm is maximum ($\approx 80 \times 10^{-4}$ mb sec^{-1}) at 500 mbs. The region of weak subsidence behind the storm (i.e. in the northeast) also shifts westward with height with a maximum value remaining in the northeast sector at all the levels. In the vertical cross section which is shown in Fig. 10e, it is seen that a vigorous upward motion is limited to a rather narrow vertical tube ahead of the depression. Maximum upward motion occurs at 500 mb. The subsidence behind the storm is relatively very weak.

We would like to mention at this point that our values of the vertical velocity appear to be largely overestimated. This is probably due to the inherent drawback in the kinematic method itself and raises a serious question about its application in preference to the diagnostic ω-equation which again has the disadvantage of being a model dependent. In any case, we feel that the emphasis here should be placed more on the distribution pattern rather than on the magnitude of the vertical velocity.

From the foregoing, it follows that the monsoon depression generates two vertical circulation cells in the northeast–southwest direction with a common limb of upward motion over the depression and two limbs of sinking motion, one in the northeast and the other in the southwest. These cells act as perturbations on the basic monsoon circulation which is essentially of Hadley type with rising motion in the north (i.e. monsoon trough) and sinking motion in the south (i.e. south of the equator). This has an important implication from the point of view of energetics because the monsoon depression, through its associated vertical circulation cells, has an energy interaction with the mean monsoon flow. A further study is already under way to examine as to what extent the mean monsoon circulation is affected by the monsoon depression in terms of energy exchange from the zonal kinetic to eddy kinetic and from zonal available to eddy available potential energy.

Cloud cover

The distribution of the total amount of clouds expressed in terms of oktas is shown in Fig. 11. For constructing the composite structure of this parameter, new sets of data consisting of additional stations which reported information of cloud cover and rainfall were utilized. In arriving at the distribution pattern shown in Fig. 11, a considerable amount of smoothing had to be invoked, especially in the regions of low cloud amount. This may be due to several factors, such as, the uncertainty of the basic data itself due to the discrete nature of this parameter and the highly subjective method of its observation. Again the influence of desert, terrain, the presence of oceans and continents would tend to distort the otherwise smooth pattern while compositing with respect to a moving depression. At any rate, the intense organization of cloud activity in front of the depression stands out conspicuously in the figure. Maximum clouding (i.e. overcast sky) is found in the southwest sector of the depression.

Precipitation

The distribution of precipitation expressed in terms of cm of rainfall in 24 hrs is presented in Fig. 12. As mentioned in the previous section, the

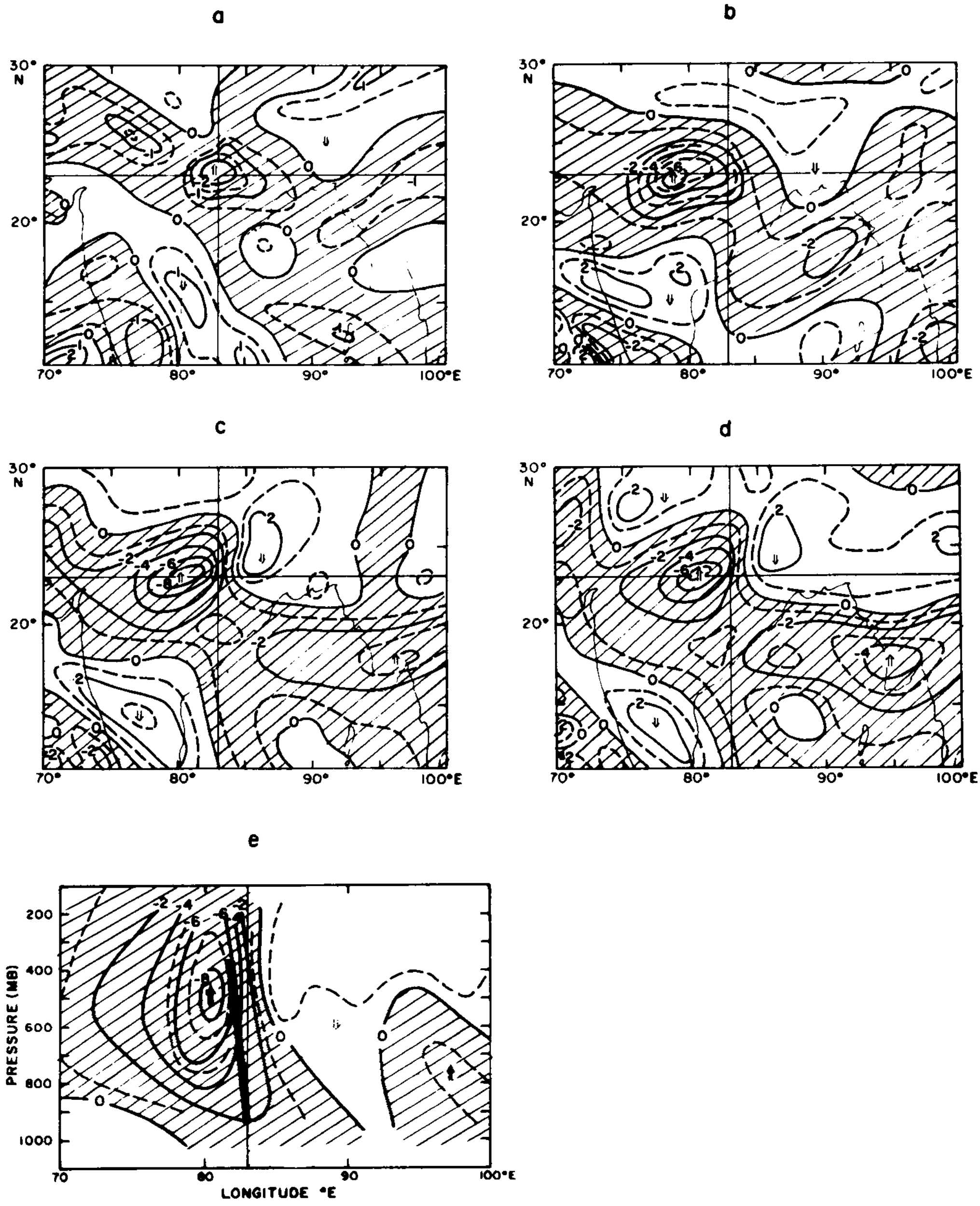

Fig. 10. The distribution of vertical velocity (10^{-5} mb sec^{-1}) at (a) 900 mb, (b) 700 mb, (c) 500 mb, (d) 300 mb, and (e) the vertical cross section of the vertical velocity along 23° N.

analysis is based on the new data sets prepared for this purpose. The most outstanding feature of Fig. 12 is that the rainfall activity due to the monsoon depression is predominantly in the southwest sector. Maximum rainfall of about 13 cm in 24 hrs occurs to the west of the depression center. The results thus confirm the earlier findings of numerous workers in this field. Referring back to Fig. 10 it is seen that the region of maximum upward motion does not coincide with that of the

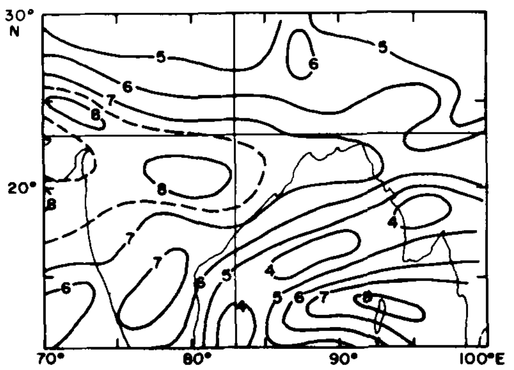

Fig. 11. The spatial distribution of the composite cloud cover (OKTA).

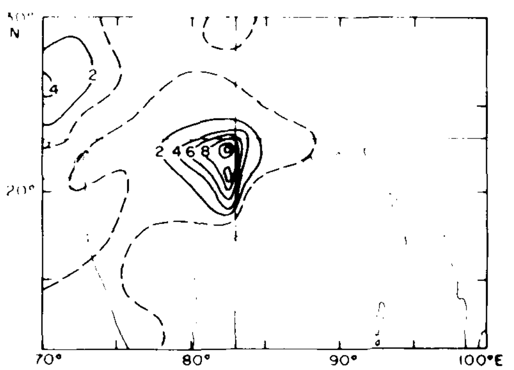

Fig. 12. The spatial distribution of the composite rainfall rate (cm/24 hr).

maximum precipitation. A one-to-one correspondence is, of course, not to be expected because the vertical velocity is on a large-scale whereas the precipitation which is primarily due to the strong convective activity (Krishnamurti et al., 1975) is on a meso-scale. Moreover, while working on the moisture budget of the depression (these results are not presented here), we noticed that the maximum import of moisture takes place in the southwest sector of the depression. This should account for the maximum rainfall in the southwest sector.

Concluding remarks

In this study, the mean picture of the monsoon depression in its complete detail is obtained using the compositing technique. The mean structure turns out to be that of an intense tropical disturbance next in class to hurricanes. The disturbance has a horizontal dimension of about 1500 km (12–14 degree longitude) and a vertical dimension of about 8 km ($\approx$400 mb). The vortex has a central pressure of 990 mb, and vigorous circulation with horizontal speeds of more than 20 m sec^{-1} are noted. The strongest winds are found in the southwest.

The associated vorticity, divergence and vertical motion fields clearly demonstrate that the strongest activity is concentrated in a narrow vertical tube ahead of the depression. This region is characterized by strong cyclonic vorticity, convergence and upward motion. Relatively weak activity is found behind the depression. Here the fields of vorticity, divergence and vertical motion are disorganized. In general, anticyclonic vorticity, divergence and subsidence are noted behind the depression.

The disturbance has a cold core structure with its vertical axis tilting eastward, which suggests that the baroclinic processes are important during its life cycle (3–5 days). The depression is accompanied by near saturation conditions ahead of it. Very moist air prevails to the southwest of the depression center. Cloudiness and precipitation are also found to be the maximum in the southwest sector of the storm.

One of the most outstanding features that is brought out by the results of the present study is that the depression is asymmetric with respect to the distributions of various parameters. More activity is concentrated in front of the depression in a rather narrow vertical tube ($\approx$300 km). The southwest sector of the depression appears to be the location of the strongest activity. Here winds, temperature, moisture, vorticity, clouding and precipitation show up with their maximum strength. In the vertical, the maximum activity is located not at the surface, but around 800 mb.

The vertical circulation induced by the monsoon depression is in the opposite direction to the mean monsoon circulation. This raises an interesting problem as to what drives this circulation and how it interacts with the mean circulation. Because of the limited size of the domain, the present study would not be able to answer these questions adequately. Further studies involving complete treatment of the energy exchange processes over a large monsoon domain are necessary to examine this aspect.

Acknowledgements

The author wishes to express his sincere thanks to Dr T. N. Krishnamurti for his continued encouragement during the course of this study. Thanks are also due to Dr Kanamitsu of NCAR and to Mr Molinari and Mr Pan for fruitful discussions.

This work was supported by the Atmospheric Sciences Section of the NSF under Grant ATM75–18945. Computer time was provided by the Florida State University.

REFERENCES

Ananthakrishnan, R. & Bhatia, K. L. 1958. Tracks of monsoon depressions and their recurvature towards Kashmir. *Symposium on Monsoons of the World.* India Meteorological Department, New Delhi, India, 157–172.

Baumhefner, D. P. 1968. Application of a diagnostic numerical model to the tropical atmosphere. *Mon. Wea. Rev. 96*, 218–228.

Bedekar, V. C. & Banerjee, A. K. 1968. A study of climatological and other rainfall patterns over central India. *Indian J. Met. Geophys. 19*, 23–30.

Das, P. K. 1952. Monsoon depressions in the Bay of Bengal. *Indian J. Met. Geophys. 3*, 225–229.

Frank, W. M. 1975. The structure and energetics of typhoons as revealed by composited rawinsonde information. *Ninth Technical Conference on Hurricanes and Tropical Meteorology* of the American Meteorological Society at Miami, Florida.

Godbole, R. V. 1975. Climatology of the Indian summer monsoon. Scientific Report No. 13, Indian Institute of Tropical Meteorology, Poona, India (in print).

Keshavmurthy, R. N. 1973. Power spectra of large-scale disturbances of the Indian southwest monsoon. *Indian J. Met. Geophys. 24*, 117–124.

Koteswaram, P. & George, C. A. 1958. A case study of a monsoon depression in the Bay of Bengal. *Symposium on Monsoons of the World.* India Meteorological Department, New Delhi, India, 145–156.

Krishnamurti, T. N., Kanamitsu, M., Godbole, R., Chang, C. B., Carr, F. & Chow, J. H. 1975. Study of a monsoon depression (Parts I and II). Rept. No. 75-3, Department of Meteorology, Florida State University, Tallahassee, Florida, 1–24 and 1–35.

Murakami, M. 1975. Analysis of summer monsoon fluctuations over India. Meteorological Research Institute, Tokyo (Manuscript to be published).

Pedgley, D. E. & Krishnamurti, T. N. 1974. Structure and behavior of a monsoon cyclone over West Africa. Rept. No. 74–2, Department of Meteorology, Florida State University, Tallahassee, Florida, 1–48.

Pisharoty, P. R. & Asnani, G. C. 1957. Rainfall around monsoon depression over India. *Indian J. Met. Geophys. 8*, 15–20.

Rao, K. V. & Rajamani, S. 1972. Study of heat sources and sinks and the generation of available potential energy in the Indian region during the southwest monsoon season. *Mon. Wea. Rev. 100*, 383–388.

Rao, Y. P. & Ramamurthy, K. S. 1968. Climatology of Indian and neighbourhood. Forecasting Manual Report No. 1–2. India Meteorological Department, Poona, India.

Reed, R. J. & Recker, E. E. 1971. Structure and properties of synoptic-scale wave disturbances in the equatorial Western Pacific. *J. Atmos. Sci. 28*, 1117–1133.

Srinivasan, V., Raman, S. & Mukherji, S. 1971. Discussion of typical synoptic weather situations. Forecasting Manual., Part III. India Meteorological Department, Poona, India, 1–68.

Tripoli, G. J. & Krishnamurti, T. N. 1975. Low level flows over the GATE area during summer, 1972. *Mon. Wea. Rev. 103*, 197–216.

Williams, K. T. 1970. A statistical analysis of satellite observed trade wind cloud clusters in the western North Pacific. Rept. No. 161, Dept. of Atmos. Sci., Colorado State University, Fort Collins, 1–80.

СОСТАВНАЯ СТРУКТУРА МУССОННОЙ ДЕПРЕССИИ

Сконструирована составная трехмерная структура муссонной депрессии с использованием пяти случаев муссонной депрессии 1973г. Рассматривались следующие параметры: ветер, температура, относительная влажность, поверхностное давление, облачный покров и осадки. Получено распределение этих элеиентов относительно центра депрессии. Результаты показывают, что депрессия представляет собою интенсивный центр низкого давления, причем давление в центре равно 990 мб. Соответствующая циркуляция весьма интенсивна. Наиболее сильные ветры, порядка 50 узлов отмечены на юго-западе. Анализ полей ветра и давления показывает, что горизонтальный масштаб депрессии составляет 1500 км. Поле температурной аномалии ясно

обнаруживает холодное ядро депрессии. Данные по осадкам показывают, что скорость выпадения дождя, превосходящая 120мм в сутки, имеет место к западу от депрессии.

Вертикальный разрез через центр депрессии, воспроизводящий ветер, указывает на то, что депрессия ограничена нижней тропосферой от поверхности до уровня 400 мб. Область впереди депрессии характеризуется сильной циклонической завихренностью, конвергенцией и восходящим движением. Остносительно слабая антициклоническая завихренность, дивергенция и опускание отмечены позади депрессии.